# Angiotensin-Converting Enzyme-2 (ACE2): Comparative Modeling of the Active Site, Specificity Requirements, and Chloride Dependence[†]

Jodie L. Guy,[‡] Richard M. Jackson,[‡] K. Ravi Acharya,[§] Edward D. Sturrock,[||] Nigel M. Hooper,[‡] and Anthony J. Turner*[,‡]

*School of Biochemistry and Molecular Biology, University of Leeds, Leeds, LS2 9JT, United Kingdom, Department of Biology and Biochemistry, University of Bath, Claverton Down, Bath, BA2 7AY, United Kingdom, and Division of Medical Biochemistry and MRC/UCT Liver Research Centre, University of Cape Town Medical School, Observatory 7925, South Africa*

*Received July 18, 2003; Revised Manuscript Received September 3, 2003*

ABSTRACT: Angiotensin-converting enzyme 2 (ACE2), a homologue of ACE, represents a new and potentially important target in cardio-renal disease. A model of the active site of ACE2, based on the crystal structure of testicular ACE, has been developed and indicates that the catalytic mechanism of ACE2 resembles that of ACE. Structural differences exist between the active site of ACE (dipeptidyl carboxypeptidase) and ACE2 (carboxypeptidase) that are responsible for the differences in specificity. The main differences occur in the ligand-binding pockets, particularly at the S2′ subsite and in the binding of the peptide carboxy-terminus. The model explains why the classical ACE inhibitor lisinopril is unable to bind to ACE2. On the basis of the ability of ACE2 to cleave a variety of biologically active peptides, a consensus sequence of Pro-X-Pro-hydrophobic/basic for the protease specificity of ACE2 has been defined that is supported by the ACE2 model. The dipeptide, Pro-Phe, completely inhibits ACE2 activity at 180 $\mu$M with angiotensin II as the substrate. As with ACE, the chloride dependence of ACE2 is substrate-specific such that the hydrolysis of angiotensin I and the synthetic peptide substrate, Mca-APK(Dnp), are activated in the presence of chloride ions, whereas the cleavage of angiotensin II is inhibited. The ACE2 model is also suggestive of a possible mechanism for chloride activation. The structural insights provided by these analyses for the differences in inhibition pattern and substrate specificity among ACE and its homologue ACE2 and for the chloride dependence of ACE/ACE2 activity are valuable in understanding the function and regulation of ACE2.

Angiotensin-converting enzyme (ACE, EC 3.4.15.1) belongs to the gluzincin family (clan MA) of metalloproteases and is a peptidyl dipeptidase with broad substrate specificity (*1*). The predominant physiological function of ACE is in cardiovascular homeostasis through cleavage of the C-terminal dipeptide from angiotensin I to produce the potent vasoconstrictor, angiotensin II. ACE[1] also inactivates the vasodilator, bradykinin, by the sequential cleavage of two C-terminal dipeptides. Two isoforms of ACE exist: somatic ACE, which has two homologous domains each containing an active site, and testicular ACE (tACE), which corresponds to the C domain of somatic ACE and has only one active site. The use of ACE inhibitors in the treatment of hypertension and heart disease has been effective for many years. For a recent review, see ref *2*.

A novel human zinc metalloprotease (ACE2/ACEH) homologous to ACE was identified by screening an EST database (*3*) and also by 5′ sequencing of a human heart failure ventricular cDNA library (*4*). ACE2 contains a single HEXXH zinc-binding motif, and other amino acid residues found to be critical for ACE activity are conserved in ACE2. ACE2 has 42% sequence identity with ACE and 61% sequence similarity in a region surrounding the active site. ACE2 transcripts are found mainly in the heart, kidney, and testis, whereas ACE mRNA expression is more widespread (*3*). Immunohistochemical studies have shown ACE2 protein predominantly in the endothelium of coronary and intrarenal vessels and in renal tubular epithelium (*4*). ACE2 differs in substrate specificity from ACE in that it functions exclusively as a carboxypeptidase. It is able to cleave a number of physiologically relevant peptides including both angiotensin I and angiotensin II as well as (des-Arg$^9$) bradykinin (*3*). However, bradykinin is not a substrate, and the classical ACE inhibitors captopril, lisinopril, and enalaprilat do not inhibit ACE2 (*3*).

ACE2 knockout mice (*ace2*$^{-/-}$), while showing no gross abnormalities and being fertile, display heart dysfunction (*5*). The *ace2* mutant mice have a severe reduction in cardiac contractility and increased angiotensin II levels, and hypoxia-induced genes are up-regulated in the heart. Interestingly, in hypertensive rats, the *ace2* gene maps to a quantitative trait locus (QTL), and ACE2 mRNA and protein expression

[†] We thank the Medical Research Council of Great Britain (MRC) (N.M.H. and A.J.T.) and the Wellcome Trust (K.R.A. and E.D.S.) for financial support. J.L.G. was supported by a MRC Ph.D. studentship.

* Corresponding author. Tel: 0113 343 3131. Fax: 0113 242 3187. E-mail: a.j.turner@leeds.ac.uk.

[‡] University of Leeds.

[§] University of Bath.

[||] University of Cape Town Medical School.

[1] Abbreviations: ACE, angiotensin-converting enzyme; Mca, (7-methoxycoumarin-4-yl)acetyl; NCPL, *N*-[(*S*)-1-carboxy-3-phenylpropyl]-L-lysine; RAS, renin-angiotensin system; rh, recombinant-human; EST, expressed sequence tag; SELDI, surface-enhanced laser desorption/ionisation; QTL, quantitative trait locus; SNPs, single nucleotide polymorphisms.

10.1021/bi035268s CCC: $25.00 
Published on Web 10/21/2003

levels were reduced as compared to normals. In addition, two single nucleotide polymorphisms (SNPs) were identified in the ACE2 locus and have been associated with a risk of cardiovascular disease in a Caucasian population (*6*).

A recent study has implicated renal ACE2 in diabetic nephropathy (*7*). ACE2 mRNA and protein expression levels were found to be reduced in the diabetic kidney. It is postulated that ACE2 is effective in diabetes via the renin-angiotensin system (RAS), a role for which has been characterized in this disease state.

The structural reasons underlying the differences in substrate specificity and inhibitor sensitivity between ACE and ACE2 are unknown. Recently, the structures of tACE (*8*) and the *Drosophila* homologue AnCE (*9*) have been elucidated. The structure of tACE was used here for comparative modeling of the active site of ACE2. This study explores the fundamental differences that exist between the active sites of ACE and ACE2 that make ACE2 a novel enzyme with unique functions.

## EXPERIMENTAL PROCEDURES

*Materials.* The peptide Mca-APK(Dnp) was synthesized by Dr. G. Knight (University of Cambridge, UK). The bradykinin-related peptide, RPPGFPSFR, was synthesized by Pepceuticals Ltd. (Leicester, UK). All other peptides were purchased from the Sigma-Aldrich Co. or Bachem Bioscience (UK) Ltd. Purified recombinant human ACE2 (rh-ACE2) was obtained from R&D Systems (Europe) Ltd. Full-length ACE was purified from pig kidney cortex as described previously (*10*).

*Homology Modeling.* The sequences of tACE and ACE2 were aligned with the program CLUSTAL W multiple sequence alignment software (ebi.ac.uk). The sequences have 42% identity in aligned regions. The coordinates of the tACE−lisinopril complex (*8*) were used to model the main chain conformation of ACE2, and the three indels (insertions/deletions) were not modeled, as they do not occur near the substrate-binding site. Side chains of tACE were replaced where necessary with those of the correct sequence in ACE2, and a multiple copy mean field refinement of side chain rotamers was performed using the modeling procedures described (*11*). The refinement was carried out in the absence of lisinopril, zinc, chloride ions, and water molecules present in the X-ray structure. The selected rotamers in the binding site were inspected for suitable atomic interactions. Only a few rotamers needed to revert to those described by the initial starting model.

*Expression of ACE2 in CHO Cells.* CHO cells were cultured in Ham's F-12 nutrient mix (Life Technologies, Inc.) supplemented with 2 mM L-glutamine, 10% (v/v) fetal bovine serum, 100 units/mL penicillin, and 100 $\mu$g/mL streptomycin at 37 °C with 5% $CO_2$. Prior to transfection (24 h), cells were seeded at a density of $1 \times 10^6$ cells per 75 $cm^2$ flask. For transient transfection, the monolayer was washed twice with Opti-MEM (Life Technologies, Inc.) before transfection with 3 $\mu$g of plasmid DNA (pTriEx 1.1 containing nucleotides 104−2323 of ACE2 cDNA encoding a truncated protein lacking the transmembrane and cytosolic domains) per flask. LipofectAMINE (Life Technologies, Inc.) was used as a cationic lipid at a ratio of DNA/lipid, 1:10 (w/w). This was added to the flasks in 2.5 mL of Opti-MEM and incubated for 16 h before the addition of Ham's F-12 nutrient mix containing 10% (v/v) fetal bovine serum. The medium was removed 24 h after the start of transfection, the monolayer was rinsed twice with Opti-MEM, and then 5 mL of Opti-MEM was added to each flask. This was incubated for a further 16 h before harvesting the medium containing soluble secreted ACE2 protein. The media samples containing protein were concentrated using 4 mL Vivaspin columns (Vivascience, Binbrook, Lincoln, UK).

*Protein Determination.* Protein concentrations were determined using the bicinchoninic acid assay with bovine serum albumin as standard (*12*).

*HPLC Analysis of Cleavage Products.* Assays for ACE2 activity were carried out in a total volume of 100 $\mu$L, containing 100 mM Tris-HCl, pH 7.4, 20 $\mu$g of protein, and 100 $\mu$M substrate. To assess the effect of chloride ions on ACE2 activity, various concentrations of NaCl were included in the assay containing 50 mM HEPES/KOH, pH 7.5 and 100 $\mu$M substrate. The buffers used in the pH dependence studies were sodium acetate, MES, HEPES, Tris, bis-Tris propane, and CAPS. For inhibition studies, compounds were preincubated with the enzyme for 30 min. Reactions were carried out at 37 °C for 2 h and stopped by heating to 100 °C for 5 min and centrifuged at 11 600*g* for 10 min. The resulting solution (75 $\mu$L) was applied to a $C_{18}$ reverse-phase HPLC column (Bondclone 10 $\mu$m, 100 × 8 mm column, Phenomenex) with a UV detector set at 214 nm. All separations were carried out at room temperature, with a flow rate of 1.5 mL/min. Mobile phase A consisted of 0.08% (v/v) phosphoric acid, and mobile phase B consisted of 40% (v/v) acetonitrile in 0.08% (v/v) phosphoric acid. A linear solvent gradient of 11−100% B over 15 min with 5 min at final conditions and 8 min reequilibration was used. The elution positions of products were determined using pure synthetic standards. The product from the cleavage of the bradykinin-related peptide and dynorphin A-(1−13) was collected and analyzed by SELDI-mass spectrometry.

*Determination of Kinetic Constants for Hydrolysis of Peptides by ACE2.* Enzyme concentration was adjusted to ensure that <15% of the substrate was consumed at the lowest substrate concentration. Under these conditions, product formation was linear with respect to time over the duration of the incubation. Substrate concentrations ranged from 20 to 200 $\mu$M, and the peak area corresponding to the product was integrated to calculate product formation. Initial velocities ($v$) were plotted versus substrate concentration and fitted to the Michaelis−Menten equation ($v = V_{max}[S]/K_m + [S]$). Turnover numbers ($k_{cat}$) were calculated from the equation $k_{cat} = V_{max}/[E]$, using an estimated ACE2 molecular mass of 120 000 Da, and the enzyme sample was assumed to be essentially pure and fully active.

*Fluorometric Assays.* Fluorogenic assays using the synthetic peptide substrate, Mca-APK(Dnp) (*15*) (final concentration 50 $\mu$M), were carried out at room temperature. The assay was monitored continuously by measuring the increase in fluorescence (excitation = 340 nm, emission = 430 nm) upon substrate hydrolysis using a Victor$^2$ fluorescence plate reader (Wallac). Initial velocities were determined from the linear rate of fluorescence increase over the 0−60 min time course. The reaction product was quantified by using standard solutions of Mca.

```
ACE2  -----------------QSTIEEQAKTFLDKFNHEAEDLFYQSSLASWNYNTNITEENVQ 60
tACE  ---------------------EAEASKFVEEYDRTSQVVWNEYAEANWNYNTNITTETSK 79
AnCE  MRLFLLALLATLAVTQALVKEEIQAKEYLENLNKELAKRTNVETEAAWAYGSNITDENEK 60
                           *  *                          * *  *** *

ACE2  NMNNAGDKWSAFLKEQSTLAQMYPLQEIQNLTVKLQLQALQQNGSSVLSEDKSKRLNTIL 120
tACE  ILLQKNMQIANHTLKYGTQARKFDVNQLQNTTIKRIIKKVQDLERAALPAQELEEYNKIL 139
AnCE  KKNEISAELAKFMKEVASDTTKFQWRSYQSEDLKRQFKALTKLGYAALPEDDYAELLDTL 120
                                    *    *            *          *

ACE2  NTMSTIYSTGKVCNPDNPQE-CLLLEPGLNEIMANSLDYNERLWAWESWRSEVGKQLRPL 179
tACE  LDMETTYSVATVCHPNGS---CLQLEPDLTNVMATSRKYEDLLWAWEGWRDKAGRAILQF 196
AnCE  SAMESNFAKVKVCDYKDSTKCDLALDPEIEEVISKSRDHEELAYYWREFYDKAGTAVRSQ 180
        *       **         * * *       *        *       *

ACE2  YEEYVVLKNEMARANHYEDYGDYWRGDYEVNGVDGYDYSRGQLIEDVEHTFEEIKPLYEH 239
tACE  YPKYVELINQAARLNGYVDAGDSWRSMYETP----------SLEQDLERLFQELQPLYLN 246
AnCE  FERYVELNTKAAKLNNFTSGAEAWLDEYEDD----------TFEQQLEDIFADIRPLYQQ 230
         ** *    *  *         *   **                *  *    ***

ACE2  LHAYVRAKLMNAY-PSYISPIGCLPAHLLGDMWGRFWTNLYSLTVPFGQKPNIDVTDAMV 298
tACE  LHAYVRRALHRHYGAQHINLEGPIPAHLLGNMWAQTWSNIYDLVVPFPSAPSMDTTEAML 306
AnCE  IHGYVRFRLRKHYGDAVVSETGPIPMHLLGNMWAQQWSEIADIVSPFPEKPLVDVSAEME 290
       * ***  *   *        *  * **** **   *        **       *    *

ACE2  DQAWDAQRIFKEAEKFFVSVGLPNMTQGFWENSMLTDPGNVQKAVCHPTAWDLGKG-DFR 357
tACE  KQGWTPRRMFKEADDFFTSLGLLPVPPEFWNKSMLEKPTDGREVVCHASAWDFYNGKDFR 366
AnCE  KQGYTPLKMFQMGDDFFTSMNLTKLPQDFWDKSIIEKPTDGRDLVCHASAWDFYLTDDVR 350
       *       *     ** *  *      **  *    *       ***  ***     * *

ACE2  ILMCTKVTMDDFLTAHHEMGHIQYDMAYAAQPFLLRNGANEGFHEAVGEIMSLSAATPKH 417
tACE  IKQCTTVNLEDLVVAHHEMGHIQYFMQYKDLPVALREGANPGFHEAIGDVLALSVSTPKH 426
AnCE  IKQCTRVTQDQLFTVHHELGHIQYFLQYQHQPFVYRTGANPGFHEAVGDVLSLSVSTPKH 410
       *  **         *** *****   *   *  * *** ***** *    **  ****

ACE2  LKSIGLLSPDFQEDNETEINFLLKQALTIVGTLPFTYMLEKWRWMVFKGEIPKDQWMKKW 477
tACE  LHSLNLLS-SEGGSDEHDINFLMKMALDKIAFIPFSYLVDQWRWRVFDGSITKENYNQEW 485
AnCE  LEKIGLLK-DYVRDDEARINQLFLTALDKIVFLPFAFTMDKYRWSLFRGEVDKANWNCAF 469
       *    **        *  ** *   **      **       **  * *   *   *

ACE2  WEMKREIVGVVEPVPHDETYCDPASLFHVSNDYSFIRYYTRTLYQFQFQEALCQAAKHEG 537
tACE  WSLRLKYQGLCPPVPRTQGDFDPGAKFHIPSSVPYIRYFVSFIIQFQFHEALCQAAGHTG 545
AnCE  WKLRDEYSGIEPPVVRSEKDFDAPAKYHISADVEYLRYLVSFIIQFQFYKSACIKAGQYD 529
       *           **       *     *         **      ****    *  *

ACE2  ------PLHKCDISNSTEAGQKLFNMLRLGKSEPWTLALENVVGAKNMNVRPLLNYFEPL 591
tACE  ------PLHKCDIYQSKEAGQRLATAMKLGFSRPWPEAMQLITGQPNMSASAMLSYFKPL 599
AnCE  PDNVELPLDNCDIYGSAAAGAAFHNMLSMGASKPWPDALEAFNGERIMSGKAIAEYFEPL 589
            **  ***     **          * **       *   *       ** **

ACE2  FTWLKDQNKNS--FVGWSTDWSPYADQSIKVRISLKSALGDKAYEWNDNEMYLFRSSVAY 649
tACE  LDWLRTENELHGEKLGWP---------------------------------------- 617
AnCE  RVWLEAENIKNNVHIGWTTSNKCVSS------------------------------- 615
        **   *        *
```

FIGURE 1: Sequence alignment of ACE2 with tACE and AnCE. Sequence alignment was carried out using CLUSTAL W multiple sequence alignment software. The zinc-binding motif and third zinc ligand are boxed. The residues that comprise the catalytic site of the enzyme (see Figure 2) are highlighted in gray. The chloride-binding residues are thickly underlined. The numbering of tACE is according to ref *8*. Those residues conserved between the three enzymes are indicated using an asterisk.

## RESULTS AND DISCUSSION

*Modeling of ACE2 and Analysis of the Active Site.* Sequence alignment of ACE2 with tACE reveals that critical active site residues in ACE are conserved in ACE2 (Figure 1). Using the ACE2 model that we have developed, it was determined whether those residues in ACE proposed to be involved in catalysis aligned with the corresponding residues present in ACE2. From the alignment, the evolutionary relationship between ACE2 and members of the ACE family is clear. A strong similarity exists between the catalytic domains such that the active site structure is highly conserved in ACE2 (Figure 2). ACE and its homologues belong to a group of metallopeptidases in which the nucleophilic attack on the scissile bond, leading to the formation of a noncovalent tetrahedral intermediate, is mediated by a water molecule. The water molecule is activated by a zinc ion, pentacoordinated by conserved protein residues and two water molecules, present in the catalytic site (*8*). Two zinc coordinating histidine residues are located within the zinc-binding motif, HEXXH; the conserved glutamate is involved in the basic attack on the substrate peptide bond. The third zinc ligand in ACE, provided by a glutamate residue, is contained within the Glu-$(Xaa)_3$-Asp motif and is separated from the second zinc ligand by a 23-residue spacer sequence. The aspartate residue within this motif serves to precisely position the first histidine zinc ligand. However, this aspartate residue is replaced by a glutamate (Glu406) in ACE2 likening ACE2 to the M9 family (clan MA), which contains microbial collagenases, with the characteristic motif Glu-$(Xaa)_3$-Glu. Williams et al. (*13*) reported that an ACE C domain mutant in which Asp991 had been replaced with Glu displayed similar enzyme kinetics to the wild type, suggesting that the replacement is truly conservative. Overall, the evidence provided by the model indicates that the catalytic mechanism of ACE2 closely resembles that of ACE.

*Classification of ACE and ACE2.* Because of the high sequence homology between ACE and ACE2, especially in the region surrounding the active site, a high confidence model of ACE2 could be built based on the recently solved structure of testicular ACE (*8*). ACE adopts an overall ellipsoid shape with a deep cleft running down the middle in which the active site lies. The ACE structure has considerable similarity with those structures solved for neurolysin (*18*) and PfuCP, the carboxypeptidase from *Pyrococcus furiosus* (*19*). Both neurolysin and PfuCP are included within the clan MX-carboxypeptidases not assigned to a clan that contain the HEXXH zinc-binding sequence rather than the characteristic HXXE motif (seen in carboxy-

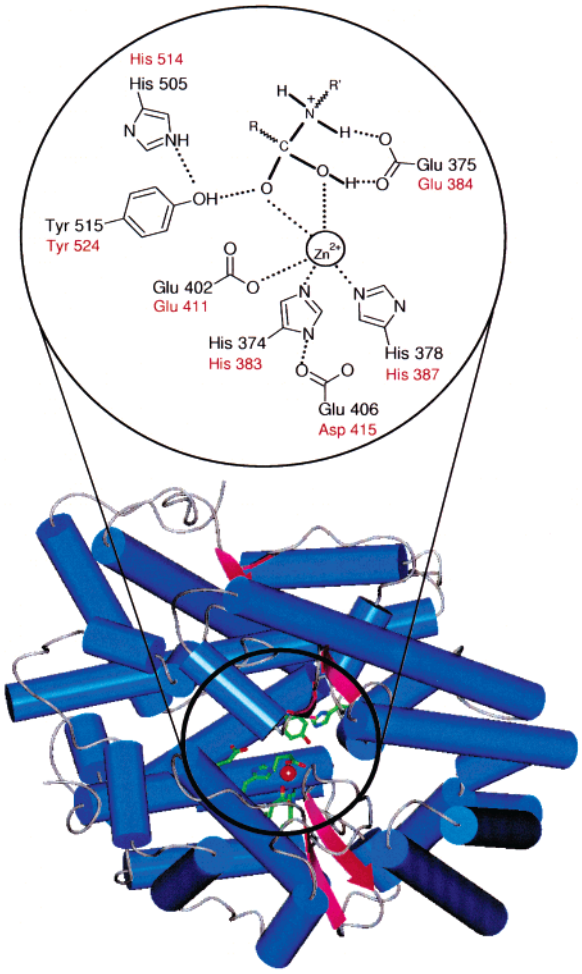


FIGURE 2: ACE2 model and a close-up schematic view of the active site. Model of the structure of ACE2 indicating the active site residues and an enlarged schematic of residues (in black) coordinating the zinc ion including the proposed reaction intermediate. The equivalent residues in tACE are noted underneath (in red). There is a single amino acid difference between the active site residues of tACE and ACE2 in that Asp415 of tACE is Glu406 in the ACE2 active site.

peptidase A). Previously, it was thought that ACE was structurally related to thermolysin and carboxypeptidase A; indeed, early ACE inhibitors were based on the active site of these enzymes (*20*−*22*). It appears now that ACE is strongly related to both neurolysin and PfuCP in its tertiary structure, grouping them together to perhaps form a new and independent clan that links their respective families. The solution of the structures of further members of these clans should allow refinement of the ever-evolving classification system of metallopeptidases (*23*). ACE2 is the first mammalian carboxypeptidase identified that contains the HEXXH zinc-binding motif likening it, in structural terms, to peptidases from the M32 family, which includes PfuCP. However, the primary sequence of ACE2 resembles that of ACE rather than PfuCP. ACE2 therefore seems to provide a link between these two, somewhat distantly related protease families. In light of recent discoveries, ACE2 structurally may form part of the same clan that not only includes its homologue ACE but also neurolysin and PfuCP.

*Comparing Substrate Specificity in the tACE and ACE2 Binding Sites.* A schematic description of protein−inhibitor interactions of the crystal structure of tACE (*8*) and the model-built structure of ACE2 are given in Figure 3A,B, respectively. The two enzymes share many common features including the conservation of residues involved in catalysis (Figure 2). It is known from the differences in substrate specificity, however, that distinct differences must exist between the active site pockets of ACE2 and ACE. ACE2 serves to remove a single residue from the C-terminus of its substrates in contrast to ACE, which primarily functions as a peptidyl dipeptidase. Subsequently, a more detailed comparison of the binding pocket of ACE and ACE2 was undertaken to investigate those residues in ACE2 responsible for such a significant difference in enzyme activity.

The main differences occur in the ligand-binding pockets, particularly at the S2′ subsite and the binding of the peptide carboxy-terminus. The cavity in tACE is larger than that of ACE2, allowing an extra amino acid to bind in the specificity pocket. In particular, tACE Gln281, which points into the binding pocket, forms a hydrogen bond with the carboxy-terminus of lisinopril (*N*-[(*S*)-1-carboxy-3-phenylpropyl]-L-lysyl-L-proline). This residue is Arg273 in ACE2, representing the insertion of an ethylene group into the side chain at this position. This causes steric conflict with the proline carboxy-terminus when the tACE conformation of lisinopril is docked into an identical position in the ACE2 model. Removing the proline carboxy-terminus allows Arg273 from the model to make a salt bridge with the lysyl carboxy-terminus of *N*-[(*S*)-1-carboxy-3-phenylpropyl]-L-lysine (NCPL). His505 and His345 of ACE2, also present in tACE (as His513 and His353), can hydrogen bond with the new carboxy-terminus. Other changes that may facilitate the switch in substrate specificity are the conversion of Lys511 and Tyr520 in tACE (which form a salt bridge and hydrogen bond, respectively, to the proline carboxy-terminus) to the non-hydrogen bonding residues Leu503 and Phe512, respectively, and conversion of Thr282 in tACE to the more bulky Phe274 in ACE2. These changes in ACE2 serve to fill out the S2′ binding pocket present in tACE. Also of note is the presence of Arg518 in ACE2, which is modeled to partially occupy the S2′ subsite but can be remodeled in a fully extended conformation to make a hydrogen bond with the lysyl carboxy-terminus of NCPL. However, it is unlikely that the guanidinium groups of Arg273 and Arg518 can simultaneously bind the carboxy-terminus due to their close proximity. The model therefore provides a rational explanation for the observed substrate specificity differences between ACE (acting as a peptidyl dipeptidase) and ACE2 (acting as a carboxypeptidase). Furthermore, with the S2′ site in ACE2 being occupied, it explains why none of the commonly used ACE inhibitors, such as lisinopril, captopril, and enalaprilat (which are based on dipeptide structures and bind in the S1′ and S2′ pockets of ACE), inhibit ACE2.

The S1′ subsite is similar in tACE and ACE2. Both contain a glutamate residue (Glu162 and Glu145, respectively) that hydrogen bonds to the lysine side chain of lisinopril in tACE as well as an aspartate residue (Asp377 and Asp368, respectively), which also forms a water-mediated hydrogen bond with the lysyl moiety. Differences occur in residues lining the pocket: Val380 in tACE to Thr371 in ACE2 is expected to be neutral given that CG2 of either side chain lines the pocket wall; however, Ala354 in tACE to Pro346 in ACE2 provides a larger nonpolar surface area of the proline side chain in ACE2. The pocket is very large in both

tACE and ACE2 and is not expected to exclude residues sterically (with the possible exception of tryptophan). This is in keeping with the observed preference in ACE2 for large hydrophobic residues or the long side chains of the positively charged Arg or Lys residues at the S1′ subsite.

The S1 subsite of ACE2 is smaller than that of tACE. The residue Phe512 (Phe504 in ACE2) is present in both cases; however, Val518 and Ser355 in tACE are replaced by the larger side chains of Tyr510 and Thr347, respectively. Thus, the carboxy-3-phenylpropyl moiety of lisinopril cannot fit sterically without readjustment of the side chain dihedral angles. The Tyr510 may be able to ring stack with a ligand proline side chain at the S1 position (not modeled). It is also possible that the smaller S1 pocket may have difficulty sterically accommodating large or C$\beta$ branched side chains.

A potent and selective ACE2 inhibitor was designed and synthesized (*14*) that has sub-nanomolar affinity for the enzyme. The scaffold (compound 1a) upon which this inhibitor was built has been modeled into the ACE2 active site model (Figure 3C) and occupies both the S1 and the S1′ subsites. The imidazole ring can sit sterically in the S1 pocket, and the leucine side chain lies in the S1′ site as seen for NCPL modeled in the ACE2 active site (Figure 3B).

*Structure−Activity Study.* To determine a structure−activity relationship for ACE2, the hydrolysis of a range of biologically active peptides was examined. Dynorphin A-(1−13), a potent endogenous agonist of the $\kappa$-opioid receptor, is hydrolyzed by ACE2. However, dynorphin A-(1−9), with a hydrophobic followed by a basic residue at the C-terminus as found in dynorphin A-(1−13) (Table 1), is not a substrate for ACE2. This may be accounted for by the absence of a proline residue in the $P_3$ position in the shorter fragment. Bradykinin is not hydrolyzed by ACE2, which may reflect the fact that the prolyl residue is in the $P_2$ position rather than in the $P_1$ or $P_3$. To investigate this possibility, a peptide was synthesized in which the proline residue in the $P_2$ position of bradykinin was swapped with the serine in the $P_3$ position (Table 1). Unlike bradykinin, this peptide was hydrolyzed by ACE2 at approximately 50% of the rate of angiotensin I. Initial inspection of the sequence of angiotensin I suggested that its hydrolysis by ACE2 might be due to the histidine ring in the penultimate $P_1$ position (Table 1), substituting for the proline moiety. However, upon reconsidering the peptide sequence, it was noted that hydrolysis could be due to the presence of a proline residue in the $P_3$ position. For some peptides, the presence of a proline residue in the $P_3$ position does not facilitate hydrolysis. This phenomenon is observed for neurotensin, neuromedin N, and kinetensin (Table 1). A common feature of these three physiological peptides is the presence of a tyrosine residue in the $P_2$ subsite. It may be, therefore, that the enzyme is unable to accommodate a large bulky residue at this position. The present study indicates that the specificity of ACE2 is dependent almost entirely upon the presence of a proline residue in either the $P_1$ or the $P_3$ position but not the $P_2$ position.

The peptidase cleavage site is generally determined by the nature of the amino acid residues within four or five positions of the scissile bond. It has been proposed that the protease specificity of ACE2 is Pro-X$_{(1-3\ \text{residues})}$-Pro-hydrophobic, where hydrolysis occurs between the proline and the hydrophobic amino acid (*15*). Overall, the data from the present study suggest that the conformation of a peptide at the C-terminus is crucial for its hydrolysis by ACE2, whose protease specificity appears rather to be Pro-X-Pro-hydrophobic/basic, where a proline residue is necessary and sufficient at either the $P_1$ or the $P_3$ position, and X can be Phe (e.g., in angiotensin I) but not Tyr (e.g., in neurotensin).

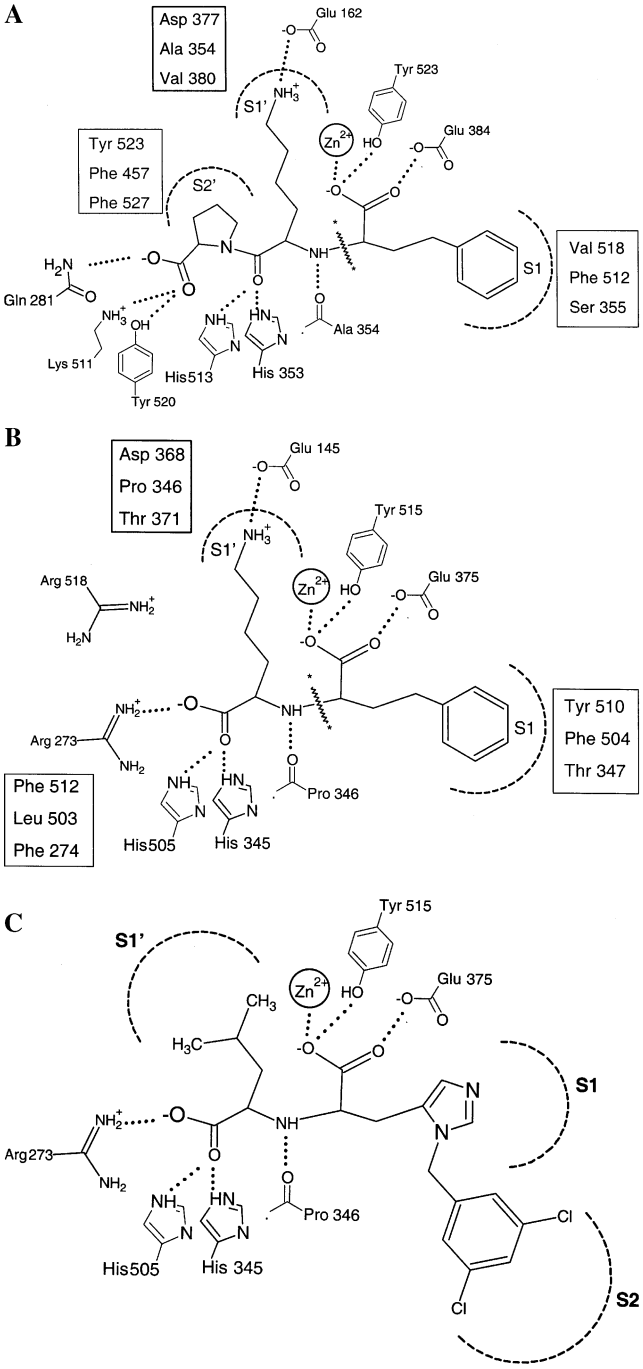


FIGURE 3: Ligand binding to ACE and ACE2. Schematic view of lisinopril binding to tACE (A) and the proposed binding of NCPL to ACE2 (B). Hydrogen bonds to the ligand are shown (dotted lines). The different binding subsites and the protein residues associated with these subsites (in boxes) are labeled. (C) Schematic view of the ACE2 inhibitor (*14*) modeled into the active site. Hydrogen bonds to the ligand are shown (dotted lines). The different binding subsites are labeled.

No systematic analysis of the effect of chain length on peptide hydrolysis by ACE2 has been carried out. We have therefore investigated the requirements using angiotensin II and its fragments (Table 2). As the peptide length shortens,

Table 1: Hydrolysis of Biologically Active Peptides by Soluble Human ACE2[a]

| | Peptide Sequence | Relative activity (%) |
|---|---|---|
| Angiotensin I | DRVYIHPFH ⇑ L | 18 |
| Angiotensin 1-9 | DRVYIHPFH | 0 |
| Angiotensin II | DRVYIHP ⇑ F | 100 |
| Angiotensin 1-7 | DRVYIHP | 0 |
| Bradykinin | RPPGFSPFR | 0 |
| Bradykinin-related | RPPGFPSF ⇑ R | 9 |
| Bradykinin-(1-8) | RPPGFSP ⇑ F | 109 |
| Bradykinin-(1-7) | RPPGFSP | 0 |
| Bradykinin-(1-5) | RPPG ⇑ F | 64 |
| Neurotensin | pELYENKPRRPYIL | 0 |
| Neurotensin-(8-13) | RRPYIL | 0 |
| Neurotensin-(1-11) | pELYENKPRRP ⇑ Y | 45 |
| Neurotensin-(1-8) | pELYENKP ⇑ R | n.d |
| Dynorphin A -(1-13) | YGGFLRRIRPKL ⇑ K | n.d |
| Dynorphin A-(1-9) | YGGFLRRIR | 0 |
| Dynorphin A-(1-8) | YGGFLRRI | 0 |
| Neuromedin N | KIPYIL | 0 |
| Kinetensin | IARRHPYFL | 0 |
| Pro-Phe | P ⇑ F | - |

[a] Detection of ACE2 peptide hydrolysis and the site of hydrolysis was determined by reverse-phase HPLC or SELDI-mass spectrometry. An arrow indicates the site of hydrolysis. Some peptides not hydrolyzed by ACE2 are shown for sequence comparison. Relative activities are represented as a percentage corresponding to the hydrolysis of angiotensin II (n.d., not determined). Hydrolysis of Pro-Phe occurs only under extensive hydrolytic conditions such that the relative activity could not be determined. pE is pyroglutamyl.

Table 2: Kinetic Constants for Hydrolysis of Angiotensin Fragments by Soluble Human ACE2[a]

| | $K_m$ ($\mu$M) | $k_{cat}$ ($s^{-1}$) | $k_{cat}/K_m$ ($\mu M^{-1}\ s^{-1}$) |
|---|---|---|---|
| angiotensin-(1−8) | 5.0 ± 0.5 | 18.5 ± 0.2 | 3.7 ± 0.05 |
| angiotensin-(3−8) | 9.1 ± 0.01 | 2.7 ± 0.06 | 0.3 ± 0.006 |
| angiotensin-(4−8) | 12.6 ± 1.2 | 1.4 ± 0.06 | 0.1 ± 0.005 |
| angiotensin-(5−8) | 24.5 ± 0.7 | 25.3 ± 0.1 | 1.0 ± 0.04 |

[a] Determinations were performed as described under Experimental Procedures using purified rh-ACE2. All determinations are $n = 3$ (for angiotensin-(3−8), $n = 2$). $K_m$ and $k_{cat}$ values are reported ±SE.

the $K_m$ value increases (approximately 5-fold between the angiotensin fragments (1−8) and (5−8)). The catalytic efficiency of ACE2 decreases, from 3.7 ± 0.05 to 0.1 ± 0.005 $\mu M^{-1}\ s^{-1}$ for angiotensin-(1−8) and angiotensin-(4−8), respectively. However, a 10-fold increase in the catalytic efficiency of ACE2 for the angiotensin-(5−8) is observed. This difference is due to an increase in the $k_{cat}$ (1.4 ± 0.06 and 25.3 ± 0.1 $s^{-1}$ for angiotensin-(4−8) and angiotensin-(5−8), respectively). It can be stated that the peptide length does not appear to be limiting for hydrolysis by ACE2, although the dipeptide angiotensin-(7−8) (Pro-Phe) is a very

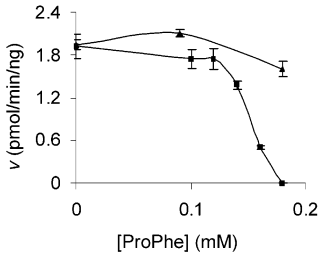


FIGURE 4: Effect of ProPhe on substrate hydrolysis by ACE2 and ACE. Activity assays were carried out as described under Experimental Procedures using purified rh-ACE2 with angiotensin II as substrate (■) or ACE with angiotensin I as substrate (▲). Enzyme activity is expressed as picomoles of product formed per minute per nanogram of pure enzyme. Product was quantified by HPLC using standards. All values are mean ± SE of three independent measurements.

poor substrate and only cleaved by ACE2 under extensive hydrolytic conditions. The kinetics of hydrolysis of angiotensin II by ACE2, which has Pro-Phe at the C-terminus, indicates that this is the best-known physiological substrate for ACE2 to date. Pro-Phe was therefore also tested as a possible inhibitor of ACE2 activity (Figure 4). The hydrolysis of angiotensin II by ACE2 is completely inhibited in the presence of 180 $\mu$M Pro-Phe. In contrast, inhibition of ACE activity is not observed over the same concentration range of the dipeptide (Figure 4). Dales et al. (*14*) designed a substrate-based ACE2 inhibitor that was built upon the C-terminal dipeptide of angiotensin I, His-Leu. However, angiotensin I is an extremely poor substrate for ACE2 with a 3.5-fold higher $K_m$ than angiotensin II (*15*). Pro-Phe might therefore represent a useful lead compound for the design of a new class of selective ACE2 inhibitors, particularly since Pro-X bonds are generally resistant to hydrolysis by other peptidases.

*Chloride Effect on ACE2 Hydrolysis.* The structure of tACE revealed the location of two buried chloride ions (*8*). The second chloride ion is bound to a water molecule and two amino acid residues, Tyr224 and Arg522. The equivalent arginine (Arg1098) in the C-domain of ACE has been reported to be essential for the chloride dependence of ACE activity (*16*). Both chloride ligands are conserved in ACE2 (Figure 1), as Tyr207 and Arg514. The ACE2 model is also suggestive of a possible mechanism for chloride ion activation. The model (built in the absence of lisinopril and all ions and solvent) predicts that Arg514 points in toward the ligand-binding site in an extended conformation in contrast to tACE in which it points away to coordinate the chloride ion. In the extended conformation, Arg514 can form a hydrogen bond with the side chain carboxyl of Glu402, which in turn coordinates the zinc ion and also the hydroxyl group of Tyr515 that is an important hydrogen donor/acceptor in peptide bond cleavage. It is possible that the two conformations of the side chain of Arg514 are both accessible and that the presence of the chloride ion influences this equilibrium. This model suggests a more direct role of Arg514 in chloride activation than has been proposed previously.

The chloride dependence of ACE is substrate-specific. We have therefore investigated whether the same phenomenon applies to ACE2. The hydrolysis of angiotensin I by ACE2 is increased by approximately 2-fold at 1 M NaCl (Figure

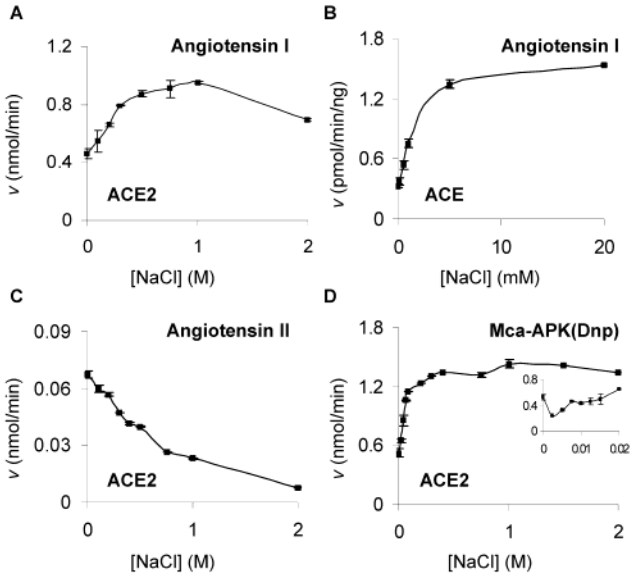


FIGURE 5: Effect of chloride ions on substrate hydrolysis by ACE2 and ACE. Activity assays were carried out as described under Experimental Procedures using recombinant ACE2 expressed in CHO cells and ACE. (A) Hydrolysis of angiotensin I by ACE2; (B) the hydrolysis of angiotensin I by ACE; (C) the hydrolysis of angiotensin II by ACE2; (D) the hydrolysis of Mca-APK(Dnp) by ACE2 with the inset graph showing ACE2 activity in the presence of lower NaCl concentrations. Enzyme activity is expressed as moles of product formed per minute. Product was quantified using pure standards. Values are means of duplicate determinations ±SE.

5A). Comparatively, the hydrolysis of angiotensin I by ACE is much more sensitive to chloride ions such that an approximately 5-fold activation is observed at 20 mM NaCl (Figure 5B). However, hydrolysis of angiotensin II by ACE2 is inhibited (Figure 5C) in the presence of chloride ions (approximately 9-fold activity decrease at 2 M NaCl). The hydrolysis of Mca-APK(Dnp) by ACE2 is greatly enhanced in the presence of chloride ions with optimal activity being reported at 1 M NaCl (*15*). At lower concentrations of salt, this effect is marked (Figure 5D). At 20 mM NaCl, ACE2 activity had increased approximately 1.2-fold, and in the presence of 80 mM NaCl, enzyme activity had increased approximately 2-fold. However, it was noted that between 0 and 10 mM NaCl the hydrolysis of Mca-APK(Dnp) by ACE2 was inhibited (Figure 5D, inset graph). In the presence of 2.5 mM NaCl, ACE2 activity had decreased by approximately 2-fold. The kinetic constants for the removal of the C-terminal lysine residue and quenching group from Mca-APK(Dnp) by ACE2 were determined in the presence and absence of 100 mM NaCl. At saturating chloride ion concentrations (100 mM NaCl), the catalytic efficiency of ACE2 was 2-fold higher than in the absence of NaCl (0.2 and 0.1 $\mu M^{-1}$ $s^{-1}$, respectively). This difference was due mainly to a decrease in the $K_m$ value between 0 and 100 mM NaCl (188.9 and 62.7 $\mu$M, respectively).

Vickers et al. (*15*) reported that in the presence of 1 M NaCl, optimal ACE2 activity was observed at pH 6.5. In this study, ACE2 activity was found to peak at approximately pH 7.0 in the presence of 300 mM NaCl (Figure 6). However, in the absence of chloride ions, ACE2 activity was optimal at pH 8.0. These data indicate that the pH dependence of ACE2 is salt dependent. Bunning and Riordan (*17*) first reported the phenomenon of the pH dependence of the anion

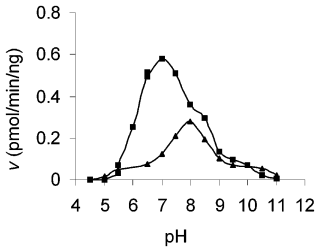


FIGURE 6: pH dependence of ACE2 proteolytic activity. Activity assays were carried out as described under Experimental Procedures using purified rh-ACE2 with Mca-APK(Dnp) as the substrate in the presence of 300 mM NaCl (■) or in the absence of NaCl (▲). Enzyme activity is expressed as picomoles of product formed per minute per nanogram of pure enzyme. Product was quantified using pure standards. Values are means of duplicate determinations.

activation of ACE in 1983. The chloride concentration at which enzyme activity is maximal increases as the pH increases.

It has been suggested that the physiological role of ACE2 could be to degrade the potent vasoconstrictor angiotensin II to produce angiotensin 1−7, which has a role in vasodilation (*3*, *2*). It is unlikely that ACE2 metabolizes angiotensin I in vivo as reflected by the low catalytic efficiency of the enzyme for this peptide (*15*). The hydrolysis of angiotensin I by ACE is activated in the presence of chloride ions, which are hence thought to exert some control within the RAS. It could be that the opposing actions of ACE and ACE2 that feature in the RAS are enhanced by this chloride effect. In the presence of chloride ions, ACE generates high levels of angiotensin II, the degradation of which by ACE2 is inhibited under similar conditions. The resulting effect would be to maintain high levels of angiotensin II in the local tissue. The mechanism underlying the substrate dependent manner of chloride activation/inhibition observed for both ACE and ACE2, however, remains unclear.

## CONCLUSION

ACE2 represents a new and potentially important target in cardio-renal disease and perhaps other diseases. The ACE2 model we present here provides an insight into the structural differences underlying the substrate specificity differences that exist between ACE and ACE2. The active site model should aid in the design of novel and specific inhibitors of ACE2 activity that may be useful pharmacological tools to explore further the physiological roles of ACE2 and to provide novel therapeutic agents.

## ACKNOWLEDGMENT

SELDI-mass spectrometry was performed by Dr. Alison Ashcroft (University of Leeds, UK). We thank Dr. Mark Parsons (University of Leeds, UK) for advice.

## REFERENCES

1. Barrett, A. J., Rawlings, N. D., and Woessner, J. F. (1998) in *Handbook of Proteolytic Enzymes* (Barrett, A. J., Rawlings, N. D., and Woessner, J. F., Eds.) pp 992−993, Academic Press, New York.
2. Turner, A. J., and Hooper, N. M. (2002) The angiotensin-converting enzyme gene family: genomics and pharmacology, *Trends Pharmacol. Sci. 23*, 177−183.
3. Tipnis, S. R., Hooper, N. M., Hyde, R., Karran, E., Christie, G., and Turner, A. J. (2000) A human homologue of angiotensin-

converting enzyme: cloning and functional expression as a captopril-insensitive carboxypeptidase, *J. Biol. Chem. 275*, 33238−33243.
4. Donoghue, M., Hsieh, F., Baronas, E., Godbout, K., Gosselin, M., Stagliano, N., Donovan, M., Woolf, B., Robison, K., Jeyaseelan, R., Breitbart, R. E., and Acton, S. (2000) A novel angiotensin-converting enzyme-related carboxypeptidase (ACE2) converts angiotensin I to angiotensin 1−9, *Circ. Res. 87*, E1−E9.
5. Crackower, M. A., Sarao, R., Oudit, G. Y., Yagil, C., Kozieradzki, I., Scanga, S. E., Oliveira-dos-Santos, A. J., da Costa, J., Zhang, L., Pei, Y., Scholey, J., Ferrario, C. M., Manoukian, A. S., Chappell, M. C., Backx, P. H., Yagil, Y., and Penninger, J. M. (2002) Angiotensin-converting enzyme 2 is an essential regulator of heart function, *Nature 417*, 822−828.
6. Chen, A. A., Barnes, G., Foti, A., Nolin, E., Lewitzky, S., Metivier, J., Meyer, J., Parker, A., and Topol, E. (2002) Two single nucleotide polymorphisms in the ACE2 locus are associated with cardiovascular disease, *Genetic Epidemiol. 23*, 272 (abstract).
7. Tikellis, C., Johnston, C. I., Forbes, J. M., Burns, W. C., Burrell, L. M., Risvanis, J., and Cooper, M. E. (2003) Characterization of renal angiotensin-converting enzyme 2 in diabetic nephropathy, *Hypertension 41*, 392−397.
8. Natesh, R., Schwager, S. L., Sturrock, E. D., and Acharya, K. R. (2003) Crystal structure of the human angiotensin-converting enzyme−lisinopril complex, *Nature 421*, 551−4.
9. Kim, H. M., Shin, D. R., Yoo, O. J., Lee, H., and Lee, J. O. (2003) Crystal structure of *Drosophila* angiotensin I-converting enzyme bound to captopril and lisinopril, *FEBS Lett. 538*, 65−70.
10. Hooper, N. M., and Turner, A. J. (1987) Isolation of two differentially glycosylated forms of peptidyl dipeptidase A (angiotensin converting enzyme) from pig brain: a reevaluation of their role in neuropeptide metabolism, *Biochem. J. 241*, 625−633.
11. Bates, P. A., Jackson, R. M., and Sternberg, M. J. (1997) Model building by comparison: a combination of expert knowledge and computer automation, *Proteins S1*, 59−67.
12. Smith, P. K., Krohn, R. I., Hermanson, G. T., Mallia, A. K., Gartner, F. H., Provenzano, M. D., Fujimoto, E. K., Goeke, N. M., Olson, B. J., and Klenk, D. C. (1985) Measurement of protein using bicinchoninic acid, *Anal. Biochem. 150*, 76−85.
13. Williams, T. A., Corvol, P., and Soubrier, F. (1994) Identification of two active site residues in human angiotensin I-converting enzyme, *J. Biol. Chem. 269*, 29430−29434.
14. Dales, N. A., Gould, A. E., Brown, J. A., Calderwood, E. F., Guan, B., Minor, C. A., Gavin, J. M., Hales, P., Kaushik, V. K., Stewart, M., Tummino, P. J., Vickers, C. S., Ocain, T. D., and Patane, M. A. (2002) Substrate-based design of the first class of angiotensin-converting enzyme-related carboxypeptidase (ACE2) inhibitors, *J. Am. Chem. Soc. 124*, 11852−11853.
15. Vickers, C., Hales, P., Kaushik, V., Dick, L., Gavin, J., Tang, J., Godbout, K., Parsons, T., Baronas, E., Hsieh, F., Acton, S., Patane, M., Nichols, A., and Tummino, P. (2002) Hydrolysis of biological peptides by human angiotensin-converting enzyme-related carboxypeptidase, *J. Biol. Chem. 277*, 14838−14843.
16. Liu, X., Fernandez, M., Wouters, M. A., Heyberger, S., and Husain, A. (2001) Arg(1098) is critical for the chloride dependence of human angiotensin I-converting enzyme C-domain catalytic activity, *J. Biol. Chem. 276*, 33518−33525.
17. Bunning, P., and Riordan, J. F. (1983) Activation of angiotensin converting enzyme by monovalent anions, *Biochemistry 22*, 110−116.
18. Brown, C. K., Madauss, K., Lian, W., Beck, M. R., Tolbert, W. D., and Rodgers, D. W. (2001) Structure of neurolysin reveals a deep channel that limits substrate access, *Proc. Natl. Acad. Sci. U.S.A. 98*, 3127−3132.
19. Arndt, J. W., Hao, B., Ramakrishnan, V., Cheng, T., Chan, S. I., and Chan, M. K. (2002) Crystal structure of a novel carboxypeptidase from the hyperthermophilic archaeon *Pyrococcus furiosus*, *Structure (Cambridge) 10*, 215−224.
20. Cushman, D. W., Cheung, H. S., Sabo, E. F., and Ondetti, M. A. (1977) Design of potent competitive inhibitors of angiotensin-converting enzyme. Carboxyalkanoyl and mercaptoalkanoyl amino acids, *Biochemistry 16*, 5484−5491.
21. Patchett, A. A., Harris, E., Tristram, E. W., Wyvratt, M. J., Wu, M. T., Taub, D., Peterson, E. R., Ikeler, T. J., ten Broeke, J., Payne, L. G., Ondeyka, D. L., Thorsett, E. D., Greenlee, W. J., Lohr, N. S., Hoffsommer, R. D., Joshua, H., Ruyle, W. V., Rothrock, J. W., Aster, S. D., Maycock, A. L., Robinson, F. M., Hirschmann, R., Sweet, C. S., Ulm, E. H., Gross, D. M., Vassil, T. C., and Stone, C. A. (1980) A new class of angiotensin-converting enzyme inhibitors, *Nature 288*, 280−283.
22. Patchett, A. A., and Cordes, E. H. (1985) The design and properties of *N*-carboxyalkyldipeptide inhibitors of angiotensin-converting enzyme, *Adv. Enzymol. Relat. Areas Mol. Biol. 57*, 1−84.
23. Rawlings, N., and Barrett, A. (1993) Evolutionary families of peptidases, *Biochem. J. 290*, 205−218.

BI035268S